J Mater Sci: Mater Electron (2023) 34:284

Effect of the electrical inhomogeneity on the magnetocapacitance sign change in the $Ho_xMn_{1-x}S$ semiconductors upon temperature and frequency variation

S. S. Aplesnin[1,2], M. N. Sitnikov[1], A. M. Kharkov[1,*], and H. Abdelbaki[1]

[1] *Reshetnev Siberian State University of Science and Technology, Krasnoyarsk, Russia*
[2] *Federal Research Center KSC SB RAS, Kirensky Institute of Physics, Krasnoyarsk, Russia*

Received: 15 October 2022
Accepted: 1 December 2022
Published online: 25 January 2023

ABSTRACT

The dielectric properties of the $Ho_xMn_{1-x}S$ ($x \leq 0.1$) semiconductors in the frequency range of $100 < \omega < 10^6$ Hz at temperatures of 80−550 K have been studied. The temperature crossover from the Debye behavior of the permittivity to the resonance behavior has been found at low holmium concentrations in the compounds. The frequency of the crossover from the migration to dipole orientation polarization with the minimum dielectric loss has been determined. The positive and negative magnetocapacitances for two concentrations of holmium ions have been found. The temperature and frequency ranges of the magnetocapacitance sign change have been established and this phenomenon has been explained using the model of the transition from electrically inhomogeneous to homogeneous states.

1 Introduction

The study of new compounds with the magnetoelectric coupling is of great practical importance, since they find wide application in microelectronic sensors. Much attention has been paid to studying multiferroics, which are characterized by a long-range magnetic and ferroelectric order [1–3]. In electrically inhomogeneous systems, the permittivity and dielectric relaxation can be enhanced due to the Maxwell−Wagner effect in the absence of the intrinsic dipole relaxation [4–6]. Magnetocapacitance without the magnetoelectric coupling can arise, if a material has the intrinsic magnetoresistance in the magnetically ordered region [7]. In particular, in the $YFeO_3$ antiferromagnet, the magnetocapacitance increases in the range of 70–300 K due to an increase in the density of carriers induced by ferrous iron [8]. The magnetocapacitance can occur without any magnetic order. In [9, 10], the position of peak the dielectric resonance a two-dimensional composite is dependent on the magnetic field, which explains the dielectric relaxation in some manganite compounds [11, 12].

Address correspondence to E-mail: khark.anton@mail.ru

https://doi.org/10.1007/s10854-022-09731-3

An urgent task is reducing dielectric loss in inhomogeneous systems. Due to the loss, the phase shift φ between a current and a voltage in various capacitive and inductive components differs from 90°. In semiconductors, the relaxation loss are due to migration polarization mechanisms and is observed in materials with random impurities or individual components in solid solutions. The contribution of the dielectric loss to the total loss of a capacitor is dominant at frequencies of about 1 MHz; therefore, the dissipation factor of ceramics is determined at these frequencies.

Along with the above-mentioned loss mechanism, there exists one more mechanism related to the absorption of the field energy by paramagnetic centers. Such centers can be rare-earth ions, as well as Ti^{3+} ions, which occur due to the oxygen deficiency. It is known well that the resonant absorption of the electromagnetic energy by paramagnetic ions can often be caused by the magnetic dipole transitions between sublevels, which are observed even in zero external magnetic field. The corresponding system of sublevels is formed by the splitting of the ground state by the crystal field [13]. In the centimeter wavelength range, perovskites exhibit a resonant decrease in the dielectric loss (tg $\varphi \sim 10^{-4}$–10^{-8}) and a high permittivity [14].

At the electromechanical resonance, oscillations of the dipole moment follow the electric field and the dissipation factor sharply drops. In the PVDF-TRFE copolymer and PZT ceramic samples, the effect of the electric polarization on the piezoelectric characteristics was studied [15]. Upon cooling after depolarization at a temperature above the Curie temperature and the disappearance of the residual polarization, the active part of the impedance decreased by an order of magnitude, while the resonance frequency did not change. This effect is explained by the rearrangement of domain structure. The resonance frequency is independent of the magnitude of the external electric field, if the latter does not exceed the coercivity.

The magnetocapacitance sign change upon heating observed in the type-2 multiferroic $HoFeWO_6$ at helium temperatures was associated to a change in the electric polarization in a magnetic field and to a strong magnetoelectric coupling [16]. In the $DyMn_{0.33}Fe_{0.67}O_3$ perovskite, both the giant positive and negative magnetodielectric coupling was found in the region of the spin-orientation transition at 290 K. The strong temperature dependence of magnetoelectric coupling and changes its sign are due to change magnetic structure from canted antiferromagnetic to collinear antiferromagnetic [17]. In the absence of magnetoelectric coupling in the paramagnetic region, the magnetocapacitance sign change has not been observed so far.

The electrically inhomogeneous states with carrier mobilities differing by an order of magnitude and with the magnetocapacitive effect can be obtained in rare-earth element-substituted manganese sulfides [18–21]. Manganese sulfide MnS is a magnetic semiconductor with a Néel temperature of 145 K [22, 23]; holmium sulfide is a semimetal with $T_N = 20$ K [24, 25]. In the $Ho_xMn_{1-x}S$ solid solutions, a reduction of the magnetic moment at the site and a slight nonlinearity of the magnetic susceptibility at 250 K for a concentration of $x = 0.05$ were found [26]. The magnetoresistance, magnetoimpedance, and electric polarization with the hysteresis vanishing at 320 K were found [27].

The our task was to obtain the relation between the magnetocapacitance and the size of the electrical inhomogeneity, which can be changed by varying the concentration and temperature.

2 Results and discussion

The $Ho_xMn_{1-x}S$ solid solutions were synthesized by melt crystallization from powdered sulfides in glassy carbon crucibles. The synthesis was described early [28]. The crystal structure of the synthesized $Ho_xMn_{1-x}S$ samples was investigated by X-ray diffractometry (XRD) on a DRON-3 diffractometer at room temperature. According to the XRD data presented in Fig. 1, the $Ho_xMn_{1-x}S$ compounds have a NaCl-type structure.

Elemental analysis of the samples was carried out on emission scanning electron microscope (Hitachi SU3500/Model3500 SEM; high-resolution electron microscope Hitachi S-5500 (SEM) and the concentrations of chemical elements are given in Table 1. The morphology of the samples presented in Fig. 2 indicates good quality.

The permittivity and dielectric loss were determined from the capacitance and loss tangent measured on AM-3028 in the frequency range of 10^2–10^6 Hz. The mechanism of the relaxation of

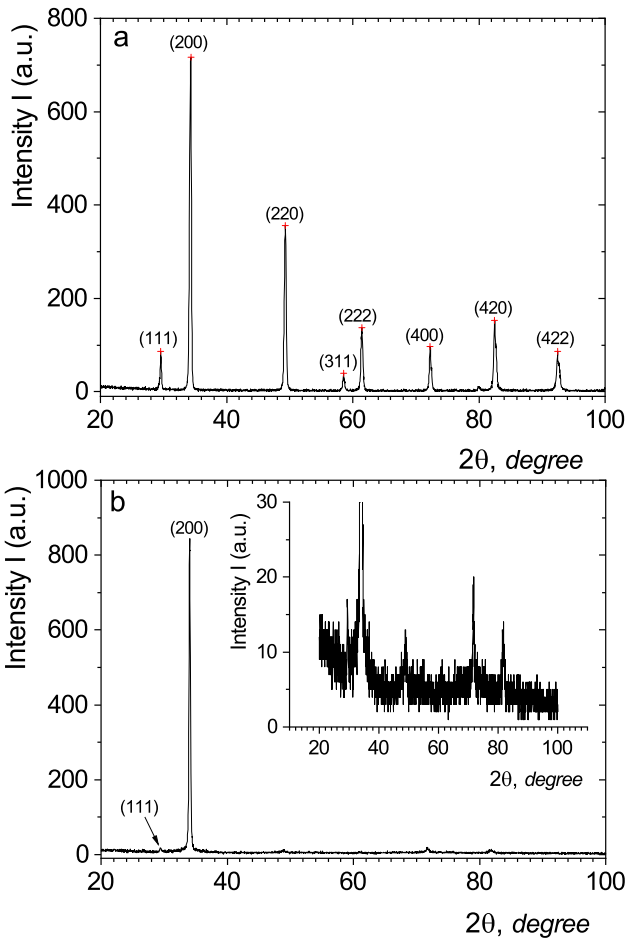

Fig. 1 X-ray diffraction patterns of $HoxMn_{1-x}S$ with $x = 0.05$ (**a**) and $x = 0.1$ (**b**) solid solutions. A decrease in the peaks with increasing concentration is related to random local deformations of the structure

polarization can be estimated from the frequency dependence of the permittivity.

The permittivity of the $Ho_{0.05}Mn_{0.95}S$ sample in the range of 80–550 K is presented in Fig. 3. Two temperature ranges, 80–240 K and 280–500 K, where the ε(ω) dependences are qualitatively different, can be distinguished. At the low temperatures ε(ω) is fitted by the Debye model with a relaxation time of $\tau = 3 \cdot 10^{-7}$ s that is corresponded to the orientational dipole polarization.

The permittivity for the $Ho_{0.05}Mn_{0.95}S$ sample have a maximum at frequencies above 0.1 MHz and temperatures of $T > 240$ K (Fig. 3b). As the temperature increases, the frequencies of the maxima shift toward higher frequencies and, when reaching $T = 380$ K, become weakly dependent on temperature (Fig. 4a).

The frequencies of the maxima of the Im(ε) and the derivative $d\mathrm{Re}(\varepsilon)/d\omega$ for the composition with $x = 0.05$ coincide. The frequency dependence of the permittivity (Fig. 5) is qualitatively different for the sample $Ho_{0.1}Mn_{0.9}S$ as compared with $x = 0.05$. The $\varepsilon(\omega)$ maximum disappears at high frequencies. The nonstoichiometric substitution by holmium causes to electron and hole doping. In the frequency range of 10^2–(10^4–10^5) Hz, the migration polarization is implemented and the permittivity components are well-described in the Debye model:

$$\mathrm{Re}(\varepsilon) = \sum_i \frac{A_i}{1 + (\omega\tau_i)^2} + \varepsilon_0 \quad (1)$$

$$\mathrm{Im}(\varepsilon) = \sum_i \frac{A_i \omega\tau_i}{1 + (\omega\tau_i)^2}, \quad (2)$$

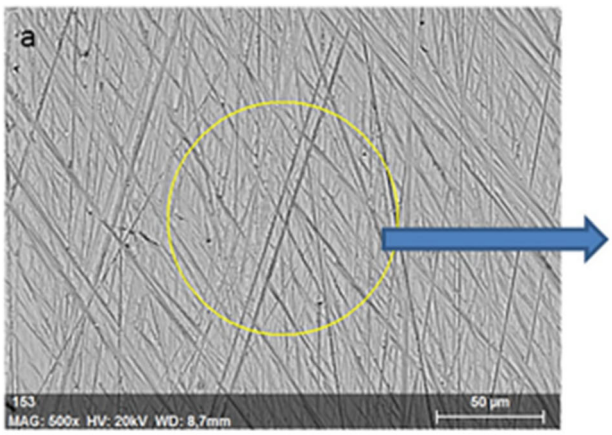

Table 1. : Point Semi-quantitative analysis of $Ho_{0.1}Mn_{0.9}S$

Element	AN	Series	norm. C [wt.%]	Atom. C [at.%]
Manganese	25	K-series	52,5	44,8
Sulfur	16	K-series	34,2	51,1
Holmium	67	L-series	13,8	4,1
		Total:	100,00	100,00

Fig. 2 SEM images for Ho0.1Mn0.9S. Table: weight ratio of elements in the sample Ho0.1Mn0.9S

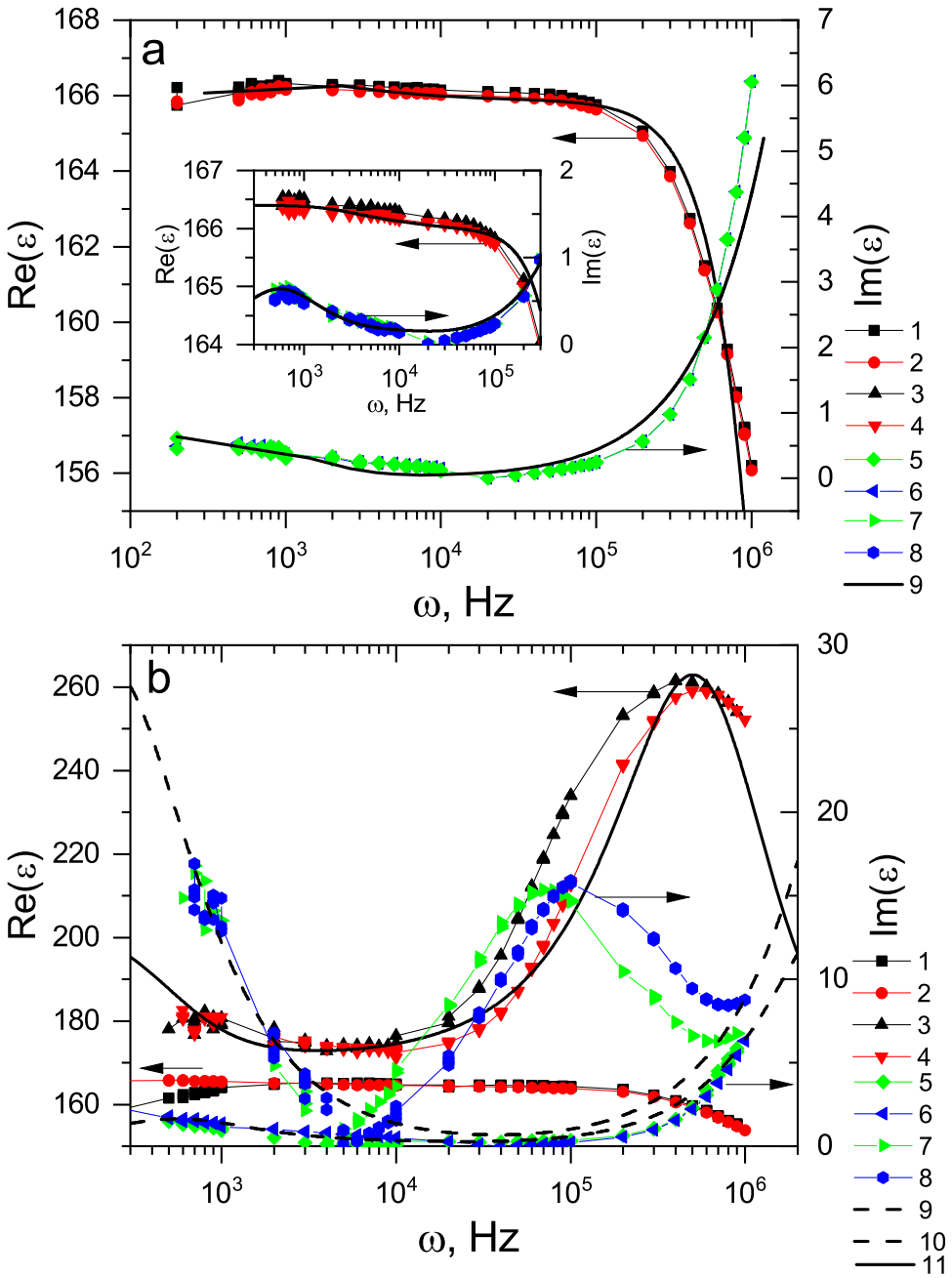

Fig. 3 Components of the complex permittivity Re(ε) (1–4) and Im(ε) (5–8) of the $Ho_xMn_{1-x}S$ with $x = 0.05$ versus frequency ω without field $H = 0$ (1,3,5,7) and in magnetic field $H = 12$ kOe (2,4,6,8) at temperatures $T = 80$ K (1,2,5,6), 160 K (3,4,7,8) (**a**); T = 240 K (1,2,5,6), 300 K (3,4,7,8) (**b**). Theoretical curves in the Debye model (9,10) and the Lorentz function (11) (**b**)

where A_i is the spectral weight. As the temperature increases, the relaxation time spectrum broadens: $\tau_1 = 3.3 \cdot 10^{-3}$ s at $T = 240$ K; $\tau_1 = 3.3 \cdot 10^{-3}$ s and $\tau_2 = 3 \cdot 10^{-4}$ s at $T = 280$ K; $\tau_1 = 1.3 \cdot 10^{-2}$ s, $\tau_2 = 4.3 \cdot 10^{-4}$ s, and $\tau_3 = 5 \cdot 10^{-6}$ at $T = 400$ K; and $\tau_1 = 2.3 \cdot 10^{-3}$ s, $\tau_2 = 3.3 \cdot 10^{-4}$ s, and $\tau_3 = 5 \cdot 10^{-6}$ s at $T = 480$ K. The relaxation time for the orientation polarization changes with temperature within $(0.7–3) \cdot 10^{-7}$ s.

The permittivity of $Ho_{0.05}Mn_{0.95}S$ is satisfactorily described by the Lorentz function in the frequency range of $(1–10) \cdot 10^4$–10^6 Hz above 240 K:

$$\mathrm{Re}(\varepsilon) = \frac{A\omega\beta}{\left[(\omega^2 - \omega_0^2)^2 + (\beta\omega)^2\right]} + \varepsilon_0 \quad (3)$$

$$\mathrm{Im}(\varepsilon) = \frac{d\mathrm{Re}(\varepsilon)}{d\omega}, \quad (4)$$

where β is the damping coefficient and ω_0 is the resonance frequency.

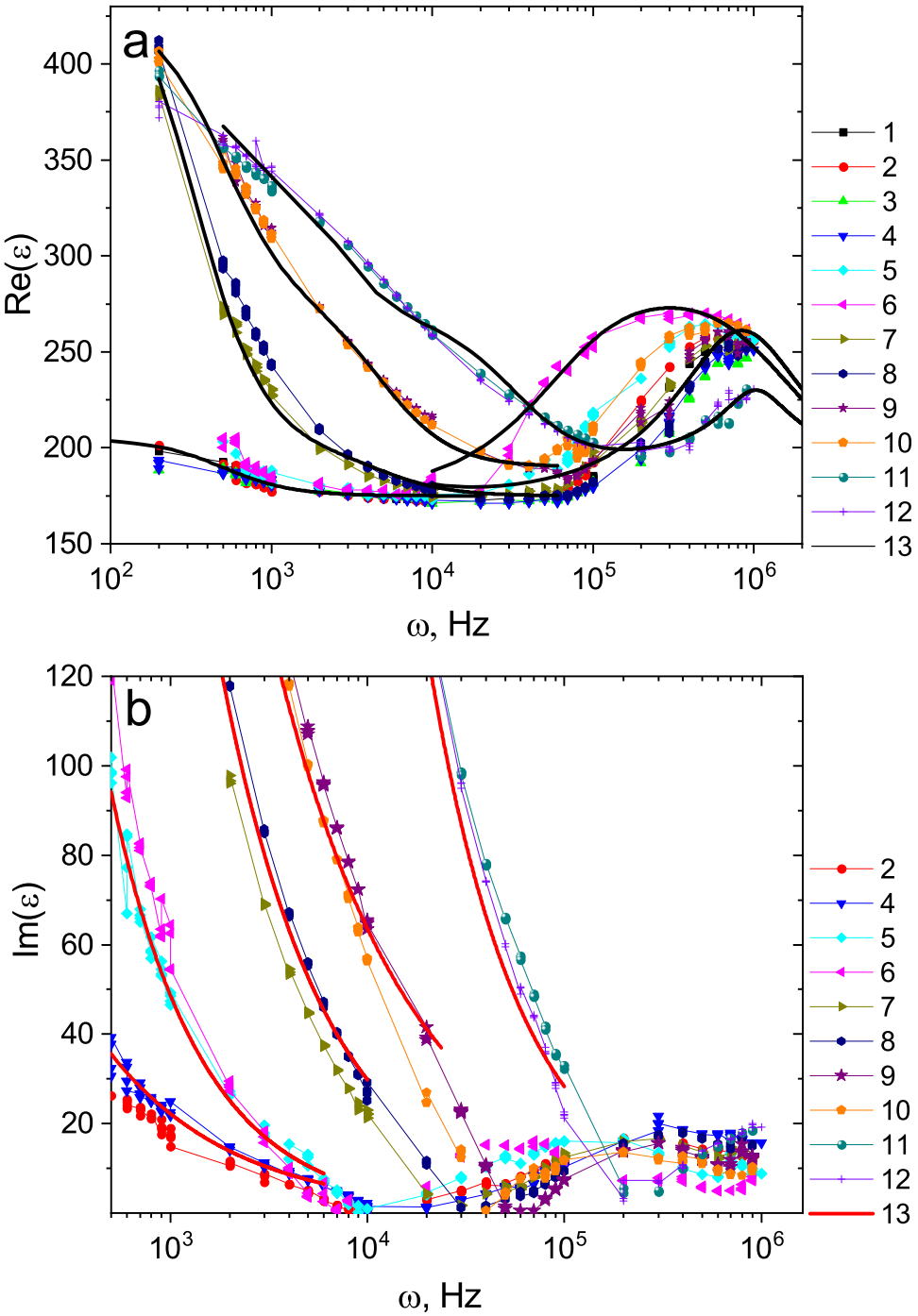

Fig. 4 Components of the complex permittivity Re(ε) (**a**) and Im(ε) (**b**) of the $Ho_xMn_{1-x}S$ with $x = 0.05$ in the resonance region without field $H = 0$ (1,3,5,7,9,11) and in magnetic field $H = 12$ kOe (2,4,6,8,10,12) versus frequency ω at temperatures $T = 340$ K (1,2), 380 K (3,4), 420 K (5,6), 460 K (7,8), 500 K (9,10), 550 K (11,12). Calculated permittivity values according to expressions (1 a, b) and (2 a, b) (solid lines 13)

The resonance can be explained by analogy with the $p-n$ junction in a diode. At a concentration of $x = 0.05$ in the matrix, the main weight comes from clusters containing one holmium ion surrounded by manganese ions. The probability of finding holmium ions surrounded by manganese ions is $c = zx(x-1)^{z-1}$ and amounts to $c = 0.34$ at $x = 0.05$. The excess electron charge of holmium ions is compensated by holes. At the Mn-S-Ho cluster interface, barrier capacitance C_b is formed, which also has ohmic resistance R and inductance L. The resonance eigen frequency of a diode is

$$\omega_{res} = \frac{1}{2\pi r C_b}\sqrt{\frac{r^2 C_b}{L} - 1}, \quad (5)$$

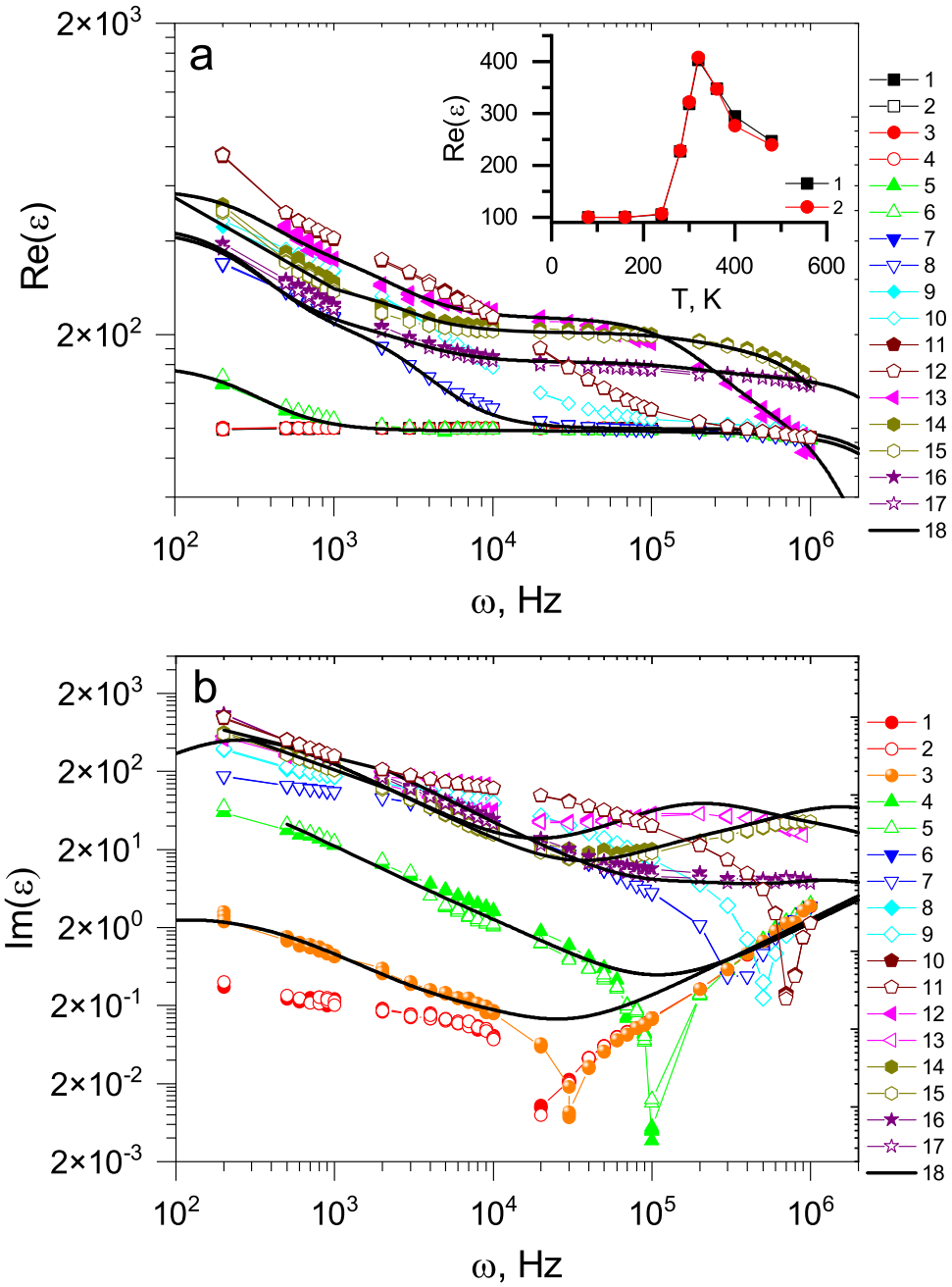

Fig. 5 Components of the complex permittivity Re(ε) (**a**) and Im(ε) (**b**) of the $Ho_xMn_{1-x}S$ with $x = 0.1$ (**a**) – in zero field $H = 0$ at temperatures T = 80 K(1), 160 K(3), 240 K(5), 280 K(7), 300 K(9), 320 K(11), 360 K(13), 400 K(14), 480 K(16), and in $H = 12$ kOe at T = 80 K(2), 160 K(4), 240 K(6), 280 K(8), 300 K(10), 360 K(12), 400 K(15), 480 K(17) versus frequency ω. (**b**) – in $H = 0$ at $T = 160$ K(1), 200 K(3), 240 K(4), 280 K(6), 300 K(8), 320 K(10), 360 K(12), 400 K(14), 480 K(16) and in $H = 12$ kOe at temperatures $T = 160$ K(2), 240 K(5), 280 K(7), 300 K(9), 320 K(11), 360 K(13), 400 K(15), 480 K(17) versus frequency ω. Fitting functions (18). Inset: The permittivity Re(ε) versus temperature without field $H = 0$ (1) and in $H = 12$ kOe (2) at frequency ω = 1000 Hz

where r is the differential resistance. The barrier capacitance C_b increases upon heating due to a decrease in the width of the electron−hole region in the vicinity of holmium ions, which leads to an increase in the resonance frequency upon heating. The minimum dissipation factor is caused by the transition from the migration relaxation to the orientational dipole relaxation. The absence of relaxation mechanisms causes to a sharp decrease in loss tangent. Above 450 K, the dielectric loss exceed the permittivity and are characteristic of relaxors with a high absorption capacity of the electromagnetic radiation [29, 30].

3 Magnetocapacitance

The capacitance and dielectric loss tangent were measured in a magnetic field of $H = 12$ kOe directed parallel to the flat capacitor plates. The magnetocapacitance was calculated as:

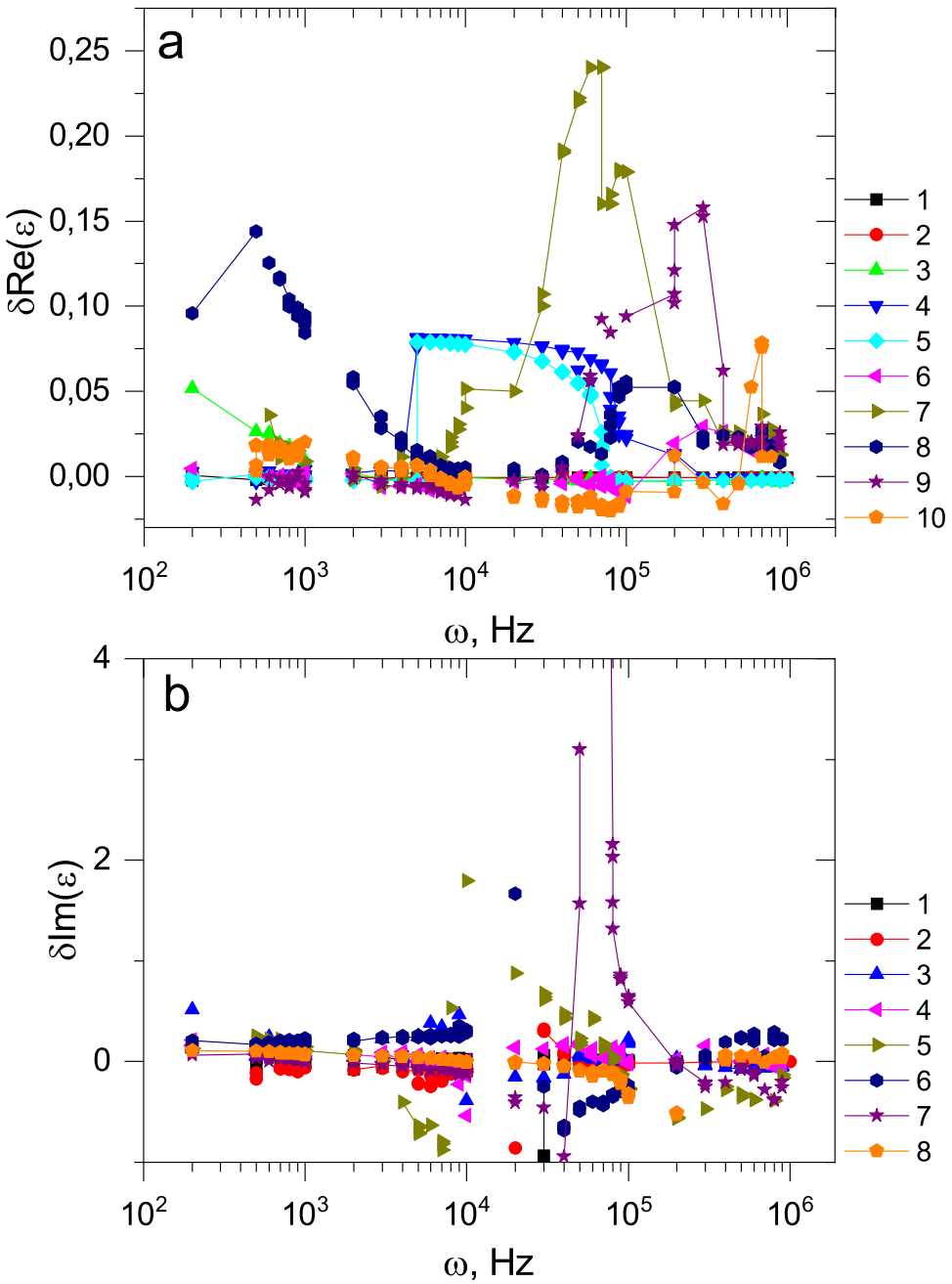

Fig. 6 Magnetocapacitance δRe(ε) for the sample $Ho_xMn_{1-x}S$ with $x = 0.05$ in the field $H = 12$ kOe at temperatures $T = 80$ K(1), 160 K(2), 240 K(3), 280 K(4), 320 K(5), 380 K(6), 420 K(7), 460 K(8), 500 K(9), 550 K (10) depend on frequency ω (**a**). The dielectric losses δIm(ε) in the field $H = 12$ kOe at temperatures $T = 80$ K(1), 160 K(2), 340 K(3), 380 K(4), 420 K(5), 460 K(6), 500 K(7), 550 K (8) versus frequency ω (**b**)

$$\delta\mathrm{Re}(\varepsilon) = \frac{\Delta\varepsilon}{\varepsilon} = \frac{(C(H) - C(0))}{C(0)} \tag{6}$$

$$\delta\mathrm{Im}(\varepsilon) = \frac{(\mathrm{Im}(\varepsilon(H)) - \mathrm{Im}(\varepsilon(0)))}{\mathrm{Im}(\varepsilon(0))}, \tag{7}$$

where $C(H)$ is the capacitance in the magnetic field and $\mathrm{Im}(\varepsilon(H)) = \mathrm{tg}\delta(H) \cdot \mathrm{Re}(\varepsilon(H))$.

The permittivity of $Ho_{0.05}Mn_{0.95}S$ above 240 K becomes larger in a magnetic field and the magnetocapacitance attains its maximum in a certain frequency range (Fig. 6a). Dielectric losses decrease at frequencies below the resonant frequency and increase above the resonant frequency in a magnetic field (Fig. 6b). An increase in the permittivity in a magnetic field is caused by the formation of deep potential wells formed by clusters with holmium ions, where the electron mobilities are strongly different from the hole mobilities in the matrix.

In the $Ho_{0.1}Mn_{0.9}S$ compound, the magnetocapacitance maximum lies in the low-frequency region and is related to the migration polarization (Fig. 7a). The permittivity increases to 4% at $T = 300$ K in a

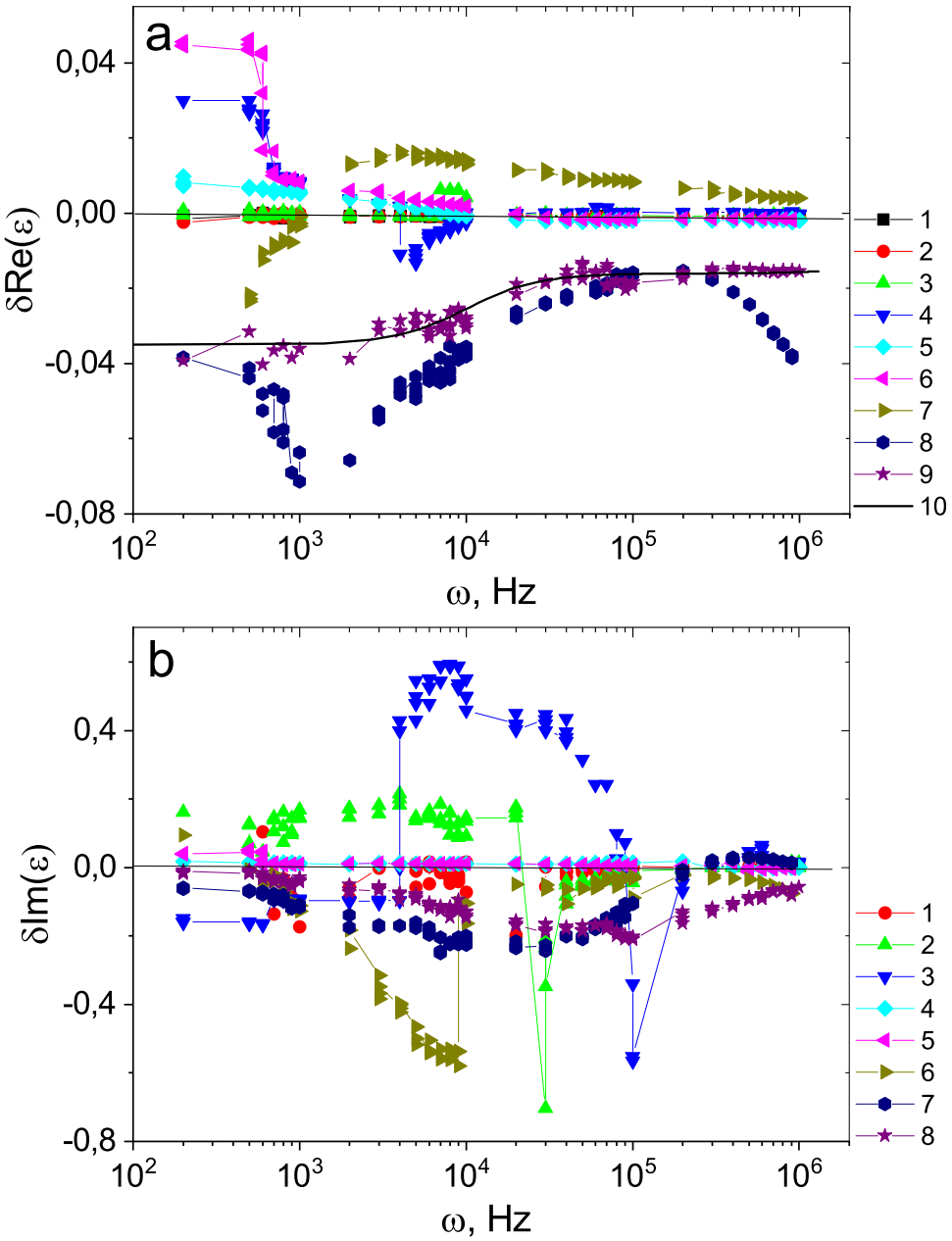

Fig. 7 Magnetocapacitance δRe(ε) for the sample $Ho_xMn_{1-x}S$ with $x = 0.1$ in the magnetic field $H = 12$ kOe at temperatures $T = 80$ K(1), 160 K(2), 200 K(3), 240 K(4), 280 K(5), 300 K(6), 360 K(7), 400 K(8), 480 K(9), fitting function (10) versus frequency ω (**a**). The dielectric losses δIm(ε) in the field $H = 12$ kOe at $T = 160$ K(1), 200 K(2), 240 K(3), 280 K(4), 300 K(5), 360 K(6), 400 K(7), 480 K(8) versus frequency ω (**b**)

magnetic field and is almost independent of the magnetic field at 320 K; at 360 K, the magnetocapacitance changes its sign from negative to positive with increasing frequency. The dielectric loss also rises in a magnetic field up to room temperature and decreases upon further heating (Fig. 7b). Upon heating, the dielectric susceptibility attains its maximum at $T = 320$ K in the range of 10^2–10^4 Hz (inset in Fig. 5), which coincides with the temperature of the disappearance of the electric polarization hysteresis [27] caused by the migration polarization.

The change in the magnetocapacitance of the $Ho_xMn_{1-x}S$ samples is described qualitatively within the magnetoelectric resonance model [9, 11]. In a two-phase two-dimensional composite medium with the limiting parameters $\partial_1 = 0$ and $\varepsilon = \varepsilon_1$, concentration x, and $\partial_2 = \partial$, $\varepsilon = 0$ with $(1 - x)$, a numerical solution was found for the complex permittivity in a two-dimensional two-component medium. In the frequency region of $\omega\tau = (0.04–0.2)$ with $x = 0.05$, an increase in the magnetocapacitance in a magnetic field was found [10], which resulted from the mixing of the

Hall resistance with the longitudinal components of the conductivity [31].

In a homogeneous system, the $\varepsilon(\omega)$ dependence changes qualitatively in a magnetic field. The change in the real part of the permittivity in a homogeneous semiconductor is described by the expression [9]:

$$\frac{\Delta\varepsilon}{\varepsilon} = -\frac{\beta^2}{(1+(\omega\tau^2))(1+\beta^2)}, \quad (8)$$

where $\beta = \mu H$, μ is the electron mobility in a magnetic field, and $\tau = RC$. In the high-temperature region, the experimental $\Delta\varepsilon/\varepsilon$ data for the $Ho_{0.1}Mn_{0.9}S$ compound are satisfactorily described by Eq. (5) with two relaxation times of $\tau = 10^{-4}$ s and $\tau = 1.5 \cdot 10^{-7}$ s. Electrical inhomogeneity causes an increase in the magnetocapacitance. In the time range of 10^{-2}–10^{-6} s in the sample with $x = 0.1$, the electrically inhomogeneous states exist up to 320 K with electron localization in potential wells. In the critical temperature range of 320–360 K, one can distinguish the time scale on which the homogeneous states with partially delocalized electrons are implemented and, in the high-frequency region, the electrical inhomogeneity is preserved, which disappears above 400 K.

In the two-dimensional model of a composite, the $\varepsilon(H)$ dependence is determined by the concentration of the conductive phase, since the Hall resistivity enhances the permittivity. A change in the concentration of current carriers in electrically inhomogeneous semiconductors will cause the magnetocapacitance sign change. In $Ho_{0.1}Mn_{0.9}S$, the resistance decreases by six orders of magnitude upon heating from 200 to 360 K, which leads to the dominance of the resistive component in the longitudinal permittivity. It is confirmed that the edge of the mobility level in $Ho_xMn_{1-x}S$ is located near the energy of localized electronic states [32]. The effective resistance increases with the field: $\rho(H) = \rho\sqrt{1+\beta^2}$ [10].

4 Conclusion

In the region of low concentrations of holmium ions in the $Ho_xMn_{1-x}S$ semiconductor, the critical temperature was found above which the permittivity has a resonance and the dielectric loss changes from the resonance to relaxation type, which was explained within the model of bound electrons and holes ($p-n$ junction) at the interface between the holmium and manganese cluster. The frequency dependence of the permittivity was described using the Debye model with the migration and orientational polarizations. At a holmium concentration of $x = 0.1$, the temperature of the maximum permittivity was found to coincide with the disappearance of the electric polarization. The growth of the permittivity and the change in the sign of dielectric loss in a magnetic field were found in a certain frequency range for the low concentrations. With increasing concentration in the $Ho_{0.1}Mn_{0.9}S$ compound, the temperature and frequency crossover from the positive to negative magnetic capacitance was found. The experiment was interpreted using the model of electrically inhomogeneous systems with different mobilities and localizations of carriers. The magnetocapacitance is positive as a result of the mixing of the Hall resistance with the longitudinal components of the conductivity. Changing the carrier density at the chemical potential level, one can increase the weight of a homogeneous system with the negative magnetocapacitance.

The existing models consider a fixed size of an inhomogeneity with different mobility of charge carriers and do not take into account changes in the concentration of charge carriers with temperature. We have shown that dielectric relaxation is described by a spectrum of relaxation times and the width of the spectrum increases with heating. In the future, these compounds can be used in microwave devices, for example, as a dielectric barrier in tunnel junctions and in spintronics.

Acknowledgements

The reported study was funded by Grant of the President of the Russian Federation № MK-620.2021.1.2. The investigation of microstructural properties of the samples was carried out using equipment's (SEM and TEM) the Krasnoyarsk Regional Center of Research Equipment of Federal Research Center «Krasnoyarsk Science Center SB RAS». The authors are grateful to A.V. Shabanov, senior researcher of the Laboratory of Molecular Spectroscopy, Kirensky Institute of Physics, for the scanning electron microscopy investigations.

Author contributions

All authors contributed to the study conception and design. Material preparation, data collection and analysis were performed by M.N.Si, A.M.K, H.A. The first draft of the manuscript was written by S.S.A and all authors commented on previous versions of the manuscript. All authors read and approved the final manuscript.

Funding

Council on grants of the President of the Russian Federation, MK-620.2021.1.2, Maksim Sitnikov.

Data availability

All data generated or analysed during this study are included in this published article [and its supplementary information files].

Declarations

Conflict of interest The authors declare that they have no known competing financial interests or personal relationships that could have appeared to influence the work reported in this paper. The authors declare the following financial interests/personal relationships which may be considered as potential competing interests.

References

1. M. Fiebig, T. Lottermoser, D. Meier, M. Trassin, Nat. Rev. Mater. **1**, 16046 (2016). https://doi.org/10.1038/natrevmats.2016.46
2. Y. Tokura, S. Seki, N. Nagaosa, Rep. Prog. Phys. **77**, 076501 (2014). https://doi.org/10.1088/0034-4885/77/7/076501
3. X. Moya, L. Hueso, F. Maccherozzi et al., Nat. Mat. **12**, 52 (2013). https://doi.org/10.1038/nmat3463
4. P. Lunkenheimer, V. Bobnar, A.V. Pronin, A.I. Ritus, A.A. Volkov, A. Loidl, Phys. Rev. B **66**, 052105 (2002). https://doi.org/10.1103/PhysRevB.66.052105
5. S. Mitra, O. Mondal, D.R. Saha, A. Datta, S. Banerjee, D. Chakravorty, J. Phys. Chem. C **115**(29), 14285 (2011). https://doi.org/10.1021/jp203724f
6. J.C. Maxwell, *Treatise on electricity and magnetism*, 3rd edn. (Dover, N.Y., 1991)
7. G. Catalan, Appl. Phys. Lett. **88**, 102902 (2006). https://doi.org/10.1063/1.2177543
8. Z.X. Cheng, H. Shen, J.Y. Xu, P. Liu, S.J. Zhang, J.L. Wang, X.L. Wang, S.X. Dou, J. Appl. Phys. **111**, 034103 (2012). https://doi.org/10.1063/1.3681294
9. M.M. Parish, P.B. Littlewood, Phys. Rev. Lett. **101**, 166602 (2008). https://doi.org/10.1103/PhysRevLett.101.166602
10. M.M. Parish, Phil. Trans. R. Soc. A **372**, 20120452 (2014). https://doi.org/10.1098/rsta.2012.0452
11. J. Rivas, J. Mira, B. Rivas-Murias et al., Appl. Phys. Lett. **88**, 242906 (2006). https://doi.org/10.1063/1.2213513
12. R.P. Rairigh, G. Singh-Bhalla, S. Tongay, T. Dhakal, A. Biswas, A.F. Hebard, Nat. Phys. **3**, 551 (2007). https://doi.org/10.1038/nphys626
13. S.A. Altshuler, B.M. Kozyrev, *Electronic paramagnetic resonance* (Science, Moscow, 1972)
14. A.G. Belous, V.I. Butko, G.N. Novitskaya, Y.M. Poplavko, E.F. Ushatkin. Fizika Tverdogo Tela **27** (7), 2013 (1985). http://mi.mathnet.ru/eng/ftt/v27/i7/p2013
15. Z. Zhang, A. Grishin, Integr. Ferroelectr. **69**(1), 401 (2005). https://doi.org/10.1080/10584580590899928
16. M. Adnani, M. Gooch, L. Deng et al., Phys. Rev. B **103**, 094110 (2021). https://doi.org/10.1103/PhysRevB.103.094110
17. F. Hong, Z. Cheng, X. Wang, J. Appl. Phys. **112**, 013920 (2012). https://doi.org/10.1063/1.4736543
18. S.S. Aplesnin, M.N. Sitnikov, JETP Lett. **100**, 95 (2014). https://doi.org/10.1134/S0021364014140021
19. S.S. Aplesnin, M.N. Sitnikov, Phys. Sol. St. **58**, 1148 (2016). https://doi.org/10.1134/S1063783416060032
20. O.B. Romanova, S.S. Aplesnin, L.V. Udod et al., J. Appl. Phys. **125**, 175706 (2019). https://doi.org/10.1063/1.5085701
21. S.S. Aplesnin, A.M. Kharkov, GYu. Filipson, Phys. Stat. Sol. B **257**, 1900637 (2020). https://doi.org/10.1002/pssb.201900637
22. S.S. Aplesnin, L.I. Ryabinkina, G.M. Abramova et al., Phys. Rev. B **71**, 125204 (2005). https://doi.org/10.1103/PhysRevB.71.125204
23. H.H. Heikens, G.A. Wiegers, C.F. van Bruggen, Sol. St. Comm. **24**, 205 (1977). https://doi.org/10.1016/0038-1098(77)91198-X
24. P.G. de Gennes, Rev. Mod. Phys. **36**, 225 (1964). https://doi.org/10.1103/RevModPhys.36.225
25. E.L. Nagaev. Fizika Tverdogo Tela **25** (12), 3617 (1983). http://mi.mathnet.ru/eng/ftt/v25/i12/p3617
26. S.S. Aplesnin, A.M. Kharkov, M.N. Sitnikov, V.V. Sokolov, JMMM **347**, 10 (2013). https://doi.org/10.1016/j.jmmm.2013.07.044

27. O.B. Romanova, S.S. Aplesnin, M.N. Sitnikov, L.V. Udod, A.M. Kharkov, Appl. Phys. A **128**, 124 (2022). https://doi.org/10.1007/s00339-021-05198-x
28. O.B. Romanova, S.S. Aplesnin, M.N. Sitnikov, L.V. Udod, JETP **132**, 831 (2021). https://doi.org/10.1134/S106377612103016X
29. L.L. Zhang, Y.N. Huang, Sci. Rep. **10**, 5060 (2020). https://doi.org/10.1038/s41598-020-61911-5
30. C.W. Ahn, C.H. Hong, B.Y. Choi et al., J. Korean Phys. Soc. **68**, 1481 (2016). https://doi.org/10.3938/jkps.68.1481
31. M.M. Parish, P.B. Littlewood, Nature **426**, 162 (2003). https://doi.org/10.1038/nature02073
32. A.M. Kharkov, M.N. Sitnikov, O.B. Begisheva, V.V. Kretinin, Hichem Abdelbaki, Nature **1614**, 012103 (2020). https://doi.org/10.1088/1742-6596/1614/1/012103